MODELING OF SEGREGATION ON MATERIAL INTERFACES BY MEANS OF THE FINITE ELEMENT METHOD

H. Ceric, A. Hoessinger, T. Binder, and S. Selberherr
Corresponding Author: H. Ceric
Vienna University of Technology
Institute for Microelectronics, Gusshausstrasse 27–29, Wien, Austria
Phone: +43(1)58801-36032, Fax: +43(1)58801-36099
email: Ceric@iue.tuwien.ac.at

Abstract. A novel approach for segregation modeling on interfaces of three-dimensional structures is described. A numerical scheme is introduced as an extension to the standard finite element scheme for the diffusion problem. A simulation example for the case of an intrinsic dopant diffusion condition is presented.

1. Introduction

The trend toward shrinking device dimensions in integrated circuits has resulted in an increased need for accurate simulation tools for process and device modeling. There are many open problems in three-dimensional finite element modeling and simulation of diffusion which is one of the most important process steps. The accurate and physically based simulation of the behavior of diffusing species on material interfaces (segregation) where species migrate between segments of different materials is one of the challenging issues in diffusion simulation [1,2,3].
This work introduces and describes a novel numerical approach for the integration of a segregation model into a finite element scheme suitable for handling diffusion models. The quality of the approach is illustrated by an example of species diffusing through two aligned cubes of different materials.

2. Physical Model

We consider two segments S_0 and S_1 of different material connected with the plane interface I. The single species with the concentration C spreads out under intrinsic dopant diffusion in both segments S_0 and S_1 with constant but different diffusivities D_0 and D_1, respectively. In that case the diffusion governing equations in each of the segments can be written as

$$D_i \Delta C = \frac{\partial C}{\partial t}, \quad i = 0, 1. \tag{1}$$

At the interface I the species flux J_{ij} from segment S_i to segment S_j (normal to the interface) is given by [2]

$$J_{ij} = h\left(C^i - \frac{C^j}{m}\right), \tag{2}$$

where h is the transport coefficient, m the segregation coefficient, and C^i and C^j are the species concentrations in segments S_i and S_j. On the outside boundaries of the S_0 and S_1, the homogenous Neumann boundary condition for the dopant species C is assumed. Segregation, i.e. mass transport of species C through the interface I, is modeled by (2) and together with (1) completes the model considered in this work.

3. Analytical Solution for One Dimension

In order to assess the numerical scheme it is useful to construct an analytical solution for a special one-dimensional case. As segment S_0 the region $x > 0$ is assumed and as segment S_1 region $x < 0$. The one-dimensional segregation problem fullfils (1) and the following initial and interface conditions

$$C_0(x, 0) = C_{init} \quad \text{for } x > 0 \quad \text{and} \quad C_1(x, 0) = 0 \quad \text{for } x < 0, \tag{3}$$

$$D_0 \frac{\partial C_0}{\partial x} = -h\left(C_1 - \frac{C_0}{m}\right), \tag{4}$$

$$D_0 \frac{\partial C_0}{\partial x} = D_1 \frac{\partial C_1}{\partial x}, \quad \text{at interface } x = 0. \tag{5}$$

Note that condition (3) also means that segments have an infinite length. We are searching for the solution of the problem given by (1), (3), (4) and (5) in the form

$$\text{for } x > 0, \quad C_0(x,t) = A_0 + B_0 C(x,t,\alpha_0, D_0) \tag{6}$$

$$\text{for } x < 0, \quad C_1(x,t) = A_1 + B_1 C(-x,t,\alpha_1, D_1) \tag{7}$$

where $A_0, A_1, B_0, B_1, \alpha_0, \alpha_1$ are constants to be determined and

$$C(x,t,\alpha,D) = \text{erfc}\left(\frac{x}{2\sqrt{Dt}}\right) - \exp\left(\frac{hx\alpha + h^2 t\alpha^2}{D}\right) \text{erfc}\left(\frac{x}{2\sqrt{Dt}} + \frac{h\sqrt{Dt}\alpha}{D}\right) \tag{8}$$

is a solution of the diffusion equation (1) for the case of the surface evaporation condition already studied in [6].

We determine constants $A_0, A_1, B_0, B_1, \alpha_0, \alpha_1$ from the initial and interface conditions (3), (4), (5) as follows. From the initial conditions we have

$$A_0 = C_{init} \quad \text{and} \quad A_1 = 0. \tag{9}$$

The interface condition (5) yields

$$\left. \frac{D_0 \frac{\partial C_0}{\partial x}}{D_1 \frac{\partial C_1}{\partial x}} \right|_{x=0} = \frac{B_0 \alpha_0}{B_1 \alpha_1} \frac{\exp\left(\frac{h^2 t\alpha_0^2}{D_0} - \frac{h^2 t\alpha_1^2}{D_1}\right) \text{erfc}\left(\frac{h\sqrt{D_0 t}\alpha_0}{D_0}\right)}{\text{erfc}\left(\frac{h\sqrt{D_1 t}\alpha_1}{D_1}\right)} = -1. \tag{10}$$

This equation is fullfiled if:

$$\frac{\alpha_0}{\sqrt{D_0}} = \frac{\alpha_1}{\sqrt{D_1}} \quad \text{and} \quad B_0 \alpha_0 = -B_1 \alpha_1. \tag{11}$$

From (4) and (9) follows

$$\left. \frac{h}{D_0} \frac{\left(C_1 - \frac{C_0}{m}\right)}{\frac{\partial C_0}{\partial x}} \right|_{x=0} = \frac{1}{\text{erfc}\left(\frac{h\sqrt{D_0 t}\alpha_0}{D_0}\right) B_0 \alpha_0} \left(B_1 \left(1 - \exp(\frac{h^2 t\alpha_1^2}{D_1}) \text{erfc}\left(\frac{h\sqrt{D_1 t}\alpha_1}{D_1}\right)\right)\right) \tag{12}$$

$$- \frac{B_0}{m} \left(1 - \exp(\frac{h^2 t\alpha_0^2}{D_0}) \text{erfc}\left(\frac{h\sqrt{D_0 t}\alpha_0}{D_0}\right)\right) - \frac{C_{init}}{m}\right) = 1 \tag{13}$$

The last equality is ensured for the condition

$$B_1 - \frac{B_0}{m} = \frac{C_{init}}{m} \quad \text{and} \quad -B_1 + \frac{B_0}{m} = B_0 \alpha_0. \tag{14}$$

By solving the equation system given by (11) and (14) we have

$$B_0 = -\frac{C_{init}}{1 + m\sqrt{\frac{D_0}{D_1}}}, \quad B_1 = \frac{C_{init}}{m + \sqrt{\frac{D_1}{D_0}}}, \quad \alpha_0 = \frac{1}{m} + \sqrt{\frac{D_0}{D_1}}, \quad \alpha_1 = 1 + \frac{1}{m}\sqrt{\frac{D_1}{D_0}}. \tag{15}$$

So we can write a solution for the problem posed by (1), (3), (4) and (5). For $x > 0$

$$C_0(x,t) = C_{init}\left(1 - \left(\frac{1}{1 + m\sqrt{\frac{D_0}{D_1}}}\right)\left(\text{erfc}\left(\frac{x}{2\sqrt{D_0 t}}\right) - \exp(\frac{hx\alpha_0 + h^2 t\alpha_0^2}{D_0})\text{erfc}\left(\frac{x}{2\sqrt{D_0 t}} + \frac{h\sqrt{D_0 t}\alpha_1}{D_0}\right)\right)\right), \tag{16}$$

and for $x < 0$

$$C_1(x,t) = \frac{C_{init}}{m + \sqrt{\frac{D_1}{D_0}}}\left(\text{erfc}\left(-\frac{x}{2\sqrt{D_1 t}}\right) - \exp(\frac{-hx\alpha_1 + h^2 t\alpha_1^2}{D_1})\text{erfc}\left(-\frac{x}{2\sqrt{D_1 t}} + \frac{h\sqrt{D_1 t}\alpha_1}{D_1}\right)\right). \tag{17}$$

4. Weak Formulation and the Basic Idea

Let us assume that the segments S_0 and S_1 are comprised with three-dimensional areas Ω_0 and Ω_1 and the connecting interface I with a two-dimensional area Θ, respectively. The tetrahedralization of areas Ω_0, Ω_1 and the triangulation of area Θ are denoted as $T_h(\Omega_0)$, $T_h(\Omega_1)$ and $T_h(\Theta)$. We discretize (1) on the element $T \in T_h(\Omega_0)$ using a linear basis function N_k. After introducing the weak formulation of (1) and subsequently applying Green's theorem we have

$$\int_T \frac{\partial C}{\partial t} N_k \, d\Omega = D_0 \int_T \Delta C \, N_k \, d\Omega = D_0 \int_\Gamma \frac{\partial C}{\partial n} N_k \, d\Gamma - D_0 \int_T \nabla C \nabla N_k \, d\Omega, \tag{18}$$

where Γ is the boundary of the element T. Assuming that $T \cap T_h(\Theta) = \Gamma_\Theta \neq \emptyset$ and marking all inside faces of T as Γ_{in} we have $\Gamma = \Gamma_\Theta \cup \Gamma_{in}$ and we can write

$$\int_\Gamma \frac{\partial C}{\partial n} N_k \, d\Gamma = \int_{\Gamma_\Theta} \frac{\partial C}{\partial n} N_k \, d\Gamma + \int_{\Gamma_{in}} \frac{\partial C}{\partial n} N_k \, d\Gamma. \tag{19}$$

In the standard finite element assembling procedure [5] we take into account only the terms $\int_T \nabla C \nabla N_k \, d\Omega$ when building up the stiffness matrix. Thereby the terms $\int_{\Gamma_{in}} \frac{\partial C}{\partial n} N_k \, d\Gamma$ do not need to be considered because of their annihilation on the inside faces.

The term $\int_{\Gamma_\Theta} \frac{\partial C}{\partial n} N_k \, d\Gamma$ makes sense only on the interface area Θ and there it can be used to introduce the influence of the species flux from the neighboring segment area Ω_1 by applying the segregation flux formula (2)

$$\int_{\Gamma_\Theta} \frac{\partial C}{\partial n} N_k \, d\Gamma = \int_{\Gamma_\Theta} h\left(C^1 - \frac{C^0}{m}\right) N_k \, d\Gamma. \tag{20}$$

After a usual assembling procedure on the tetrahedralization $T_h(\Omega_0)$ and $T_h(\Omega_1)$ has been carried out and the global stiffness matrix for both segment areas of the problem (1) has been built, the interface inputs (20) for the segregation fluxes J_{01} and J_{10} are evaluated on the triangulation $T_h(\Theta)$ and assembled into the global stiffness matrix according to the particular *assembling algorithm* developed in this work.

5. Finite element Approximation and Assembling Algorithm

The numerical implementation of the concept described in Section 4. is carried out in two steps.
Step 1.
We assemble the general matrix $\mathbf{G}$ of the problem for both segment, i.e., for both diffusion processes. The number of points in segments S_0 and S_1 is denoted as s_0 and s_1, respectively. The general matrix has dimensions $(s_0 + s_1) \times (s_0 + s_1)$ and the inputs are correspondingly indexed. The matrix is assembled by distributing the inputs from matrix $\mathbf{\Pi_i}(T_i)$, $dim(\mathbf{\Pi_i}(T_i)) = 4 \times 4$, defined for each $T_i \in T_h(\Omega_i)$, $i = 0, 1$

$$\mathbf{\Pi_i}(T_i) = \mathbf{K}(T) + D_i \Delta t \mathbf{M}(T_i) \tag{21}$$

Δt is the time step of the discretisized time, and $\mathbf{K}(T_i)$ and $\mathbf{M}(T_i)$ are stiffness and mass matrix defined on single tetrahedra T_i from $T_h(\Omega_i)$

$$K_{pq}(T_i) = \int_T \nabla N_p \nabla N_q \, dx \, dy \, dz$$

$$M_{pq}(T_i) = \int_T N_p N_q \, dx \, dy \, dz \quad p, q \in \{0, 1, 2, 3\}. \tag{22}$$

Let us denote vertices of the element T_i from the tetrahedralization $T_h(\Omega_i)$ by P_0, P_1, P_2, P_3 and their indexes in the segment S_i by $0 \leqslant k_{P_0}^i, k_{P_1}^i, k_{P_2}^i, k_{P_3}^i < s_i$. Assembling means, for each $T_i \in T_h(\Omega_i)$, and $r, q \in \{0, 1, 2, 3\}$ adding the term $\mathbf{\Pi_i}(r, q)$ to $\mathbf{G}(i \, s_0 + k_{P_r}^i, i \, s_0 + k_{P_q}^i)$.

After this assembling procedure is carried out the general matrix $\mathbf{G}$ has following the structure:

$$\mathbf{G} = \begin{bmatrix} \mathbf{S_{00}} & \mathbf{0} \\ \mathbf{0} & \mathbf{S_{11}} \end{bmatrix} \tag{23}$$

Where $dim(\mathbf{S_{00}}) = s_0 \times s_0$ and $dim(\mathbf{S_{11}}) = s_1 \times s_1$. The matrix $\mathbf{S_{00}}$ and $\mathbf{S_{11}}$ are the finite element discretizations of the equation (1) for the segments S_0 and S_1, respectively.

Step 2.

For the element $T_0 \in T_h(\Omega_0)$ with one of its faces (Γ_Θ) laying on the interface I according to the idea presented in the Section 4. the weak formulation is:

$$\int\limits_{T_0} \frac{\partial C}{\partial t}\, N_k\, d\Omega = \int\limits_{\Gamma_\Theta} h\left(C^1 - \frac{C^0}{m}\right) N_k\, d\Gamma - D_0 \int\limits_{T_0} \nabla C \nabla N_k\, d\Omega, \qquad (24)$$

The segregation term on the right side of (24) is evaluated on the two-dimensional element Γ_Θ.

Now if we discretise (24) by applying the idea presented in Section 5 and taking a *backward Euler* time scheme with time step Δt we have for the segment S_0:

$$\mathbf{M}(T_0)\left(C_0^n - C_0^{n-1}\right) = h\Delta t\, \mathcal{M}\left(C_1^n - \frac{1}{m}C_0^n\right) - D_0 \Delta t\, \mathbf{K}(T_0)C_0^n. \qquad (25)$$

where $C_0^n = (C_{0,P_0}^n, C_{0,P_1}^n, C_{0,P_2}^n, C_{0,P_3}^n)^T$ and $C_0^{n-1} = (C_{0,P_0}^{n-1}, C_{0,P_1}^{n-1}, C_{0,P_2}^{n-1}, C_{0,P_3}^{n-1})^T$ are the values of the species concentration for the nth and $n - 1^{st}$ time step at the vertices of element T_0 and analogously $C_1^n = (C_{1,P_0}^n, C_{1,P_1}^n, C_{1,P_2}^n, C_{1,P_3}^n)^T$ for $T_1 \in T_h(\Omega_1)$, $T_0 \cap T_1 = \Gamma_\Theta$. Without losing generality we assume that vertices P_3 of the tetrahedas T_0 and T_1 is the point which doesn't belong to the interface Θ. In that case matrix $\mathcal{M}$ from (25) has a simple structure

$$\mathcal{M} = det(J(\Gamma_\Theta))/24 \begin{bmatrix} 2 & 1 & 1 & 0 \\ 1 & 2 & 1 & 0 \\ 1 & 1 & 2 & 0 \\ 0 & 0 & 0 & 0 \end{bmatrix}, \qquad (26)$$

where $J(\Gamma_\Theta)$ is the Jacobian evaluated on the element Γ_Θ.

With (21) we obtain

$$\mathbf{\Pi_0}(T_0)\, C_0^n - h\Delta t\, \mathcal{M}\left(C_1^n - \frac{1}{m}C_0^n\right) = \mathbf{M}(T_0)\, C_0^{n-1} \qquad (27)$$

Let us introduce now $\mathbf{H_0}(\Gamma_\Theta) = -\frac{h}{m}\Delta t\, \mathcal{M}$ and $\mathbf{H_1}(\Gamma_\Theta) = h\Delta t\, \mathcal{M}$ and write for the element T_0

$$\mathbf{\Pi_0}(T_0)\, C_0^n - \mathbf{H_0}(\Gamma_\Theta)\, C_0^n - \mathbf{H_1}(\Gamma_\Theta)\, C_1^n = \mathbf{M}(T_0)\, C_0^{n-1} \qquad (28)$$

and analogously for the element T_1

$$\mathbf{\Pi_1}(T_1)\, C_1^n + \mathbf{H_0}(\Gamma_\Theta)\, C_0^n + \mathbf{H_1}(\Gamma_\Theta)\, C_1^n = \mathbf{M}(T_1)\, C_1^{n-1}. \qquad (29)$$

In the following text, for the sake of simplicity, we omit Γ_Θ from $\mathbf{H_i}(\Gamma_\Theta)$ and write $\mathbf{H_i}$.

The contributions of $\mathbf{\Pi_0}(T_0)$ and $\mathbf{\Pi_1}(T_1)$ are already included in the general matrix $\mathbf{G}$ by the assembling procedure made in the first step, the build up of $\mathbf{G}$ can now be completed by adding the inputs from matrix $\mathbf{H_0}$ and $\mathbf{H_1}$ in order to take into account segregation on the interface I.

Let us denote the vertices of the element $\Gamma_\Theta \in T_h(\Theta)$ as P_0, P_1, P_2. In the tetrahedralization $T_h(\Omega_0)$ these points have indices $0 \leqslant k_{P_0}^0, k_{P_1}^0, k_{P_2}^0 < s_0$ and indices $0 \leqslant k_{P_0}^1, k_{P_1}^1, k_{P_2}^1 < s_1$ in the tetrahedralization $T_h(\Omega_1)$. The actual implementation of the scheme (28) at for each element Γ_Θ of the interface triangulation $T_h(\Theta)$ and for $r, q \in \{0, 1, 2, 3\}$:

- adding the term $-\mathbf{H_0}(r, q)$ to the input $\mathbf{G}(k_{P_r}^0, k_{P_q}^0)$

- adding the term $-\mathbf{H_1}(r, q)$ to the $\mathbf{G}(k_{P_r}^0, s_0 + k_{P_q}^1)$

- adding the term $\mathbf{H_0}(r, q)$ to $\mathbf{G}(s_0 + k_{P_r}^1, k_{P_q}^0)$

- adding the term $\mathbf{H_1}(r, q)$ to the $\mathbf{G}(s_0 + k_{P_r}^1, s_0 + k_{P_q}^1)$.

After that the assembling of the general matrix $\mathbf{G}$ is completed. These procedure is carried out at each time step of the simulation.
Let us take:

$$\mathbf{c^n} = (C_{0,0}^n, C_{0,1}^n, ..., C_{0,s_0}^n, C_{1,0}^n, C_{1,1}^n, ..., C_{1,s_1}^n),$$
$$\mathbf{c^{n-1}} = (C_{0,0}^{n-1}, C_{0,1}^{n-1}, ..., C_{0,s_0}^{n-1}, C_{1,0}^{n-1}, C_{1,1}^{n-1}, ..., C_{1,s_1}^{n-1}). \tag{30}$$

Evaluating the species concentration at the nth time step in both segments including segregation on the interface is performed by solving the following linear equation system:

$$\mathbf{G}\,\mathbf{c^n} = \mathbf{M}\,\mathbf{c^{n-1}}. \tag{31}$$

$\mathbf{M}$ in the last equation denotes the global stiffness matrix assembled from the element stiffness matrix $\mathbf{M}(T_0)$ evaluated on each element T from the tetrahedralizations $T_h(\Omega_0)$ and $T_h(\Omega_1)$.

$n = 20,\ m = 3$

$n = 80,\ m = 3$

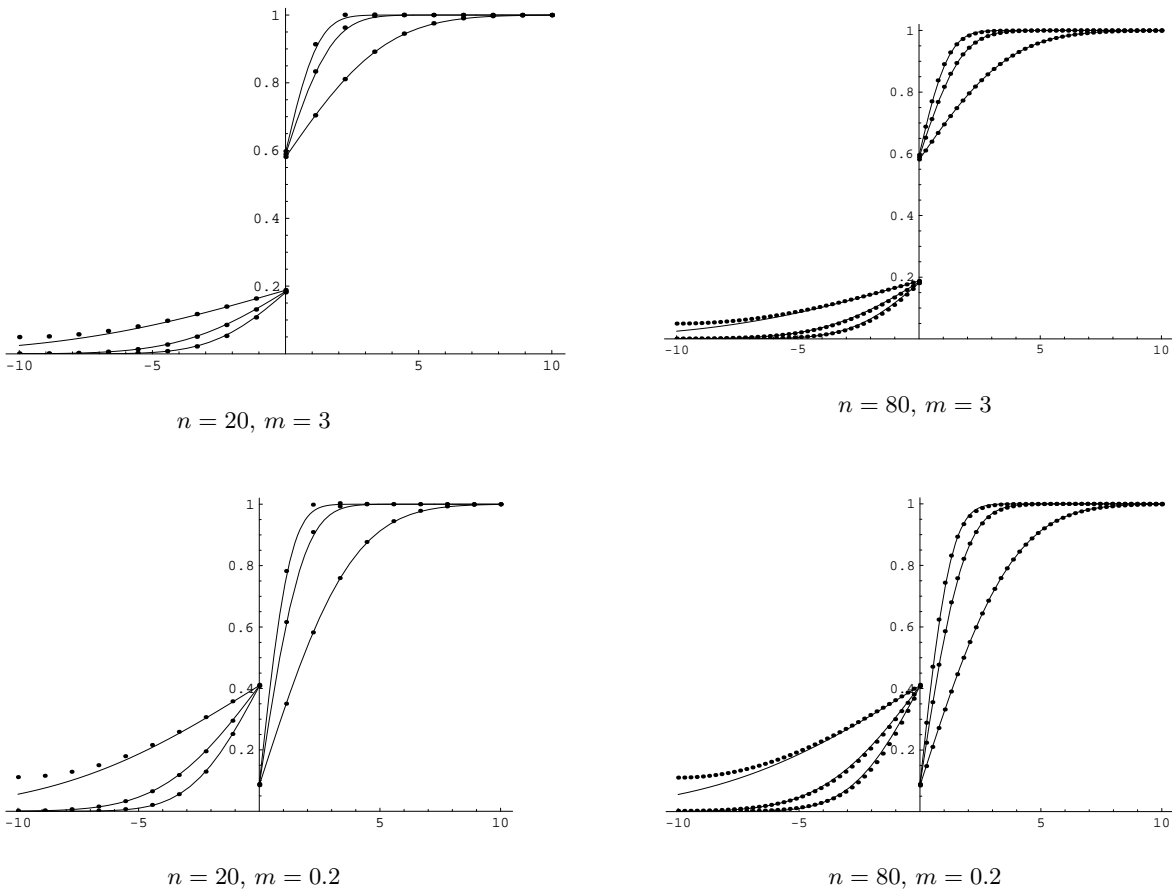$n = 20,\ m = 0.2$

$n = 80,\ m = 0.2$

Figure 1: The comparison between numerical (points) and analytical solution (full line) for three different time steps in each figure above. Because of the assumption of infinite media for the derivation of the analytical solution there is a deviation of the solution from the numerical one in the proximity of the point -10 on the abscissa.

6. Simulation Results

6.1. Comparison between Analytical Solution and One-Dimensional Numerical Scheme

In order to confirm our numerical scheme and to investigate its behavior for several cases of model parameters we compare the one-dimensional version of the scheme with the analytical solution given in

Section 3. We use the nodal error e_{L_∞} to give a measure of the quality of the finite element solution:

$$e_{L_\infty} = |C - C^h|_{L_\infty} = \sqrt{\frac{1}{n} \sum_{0 \le i < n} [C^h(i\,\Delta x, t) - C(i\,\Delta x, t)]^2} \tag{32}$$

Where C is the analytical solution given by (16) and (17) and C^h is the finite element approximation described in Section 5. reduced to the one-dimensional case, n is the number of the nodes of the equidistant spatial discretization. The evaluation was carried out for $C_{init} = 1.0$, $D_0 = 0.1$, $D_1 = 0.5$, $m = 0.2$, $h = 2$ and simulation time $t_{end} = 5$.

For $\Delta t = 1$

number of nodes	10	20	40
nodal error e_{L_∞}	0.035865	0.007957	0.007011

and for $\Delta t = 0.1$

number of nodes	10	20	40
nodal error e_{L_∞}	0.033980	0.006920	0.001720

As we can see from the tables above an error improvement due to finer spatial discretization is more distinctive for the smaller time step. Fig.1 illustrate the quality of the numerical scheme for two different discretisations ($n = 20$ and $n = 80$) and for two different segregations coefficients $m = 0.2$ and $m = 3$. Each picture shows diffusion profiles on material interfaces for simulation time $t = 5$, $t = 10$, and $t = 45$. The analytical solution was constructed assuming infinite diffusion media, therefore the comparison is justifiable only for the undisturbed edges of the simulation area. These assumption is the cause of differences between the numerical and the analytical solution for the values around $x = -10$ in Fig.1.
As we can see from Fig.1 the numerical scheme produces results which very accurately correspond to the analytical solution. The numerical solution follows already for the rough discretization the analytical solution. For the purpose of this comparison a one-dimensionel finite element scheme for the diffusion equation and segregation was implemented.

6.2. 3D Example

The finite element model for equation (1) and the accompanying segregation model (2) has been implemented in our tree-dimensional object oriented PDE solver. In order to demonstrate the applicability of the presented scheme for three-dimensional segregation simulation we carried out a numerical experiment for the case of two cubes with a common plane rectangular interface. Initial species distribution has higher concentration Gaussian profile in top cube and lower constant concentration in the bottom (Fig.2, $t = 0$) cube. Simulation shows that the species penetrates from the top cube into the bottom cube (Fig.2, $t = 2, 5, 10$) at the rate controllable by segregation and the transport coefficient. The example of simulated species diffusion exhibits accurate physical behavior on the material interface. The calculation of the species mass in both segments has shown that the presented numerical scheme complies with the mass conservation law very well.

7. Conclusion

We presented an extension of the common finite element scheme for the diffusion equations which makes possible numerical simulation of the segregation effect on the material interface for one-,two- and three-dimensional geometries. A rigorous foundation of the basic concept is given. For the one-dimensional case an analytical solution of the problem is derived. The results of the numerical procedure are evaluated with the analytical solution with which it exhibits very good agreement.

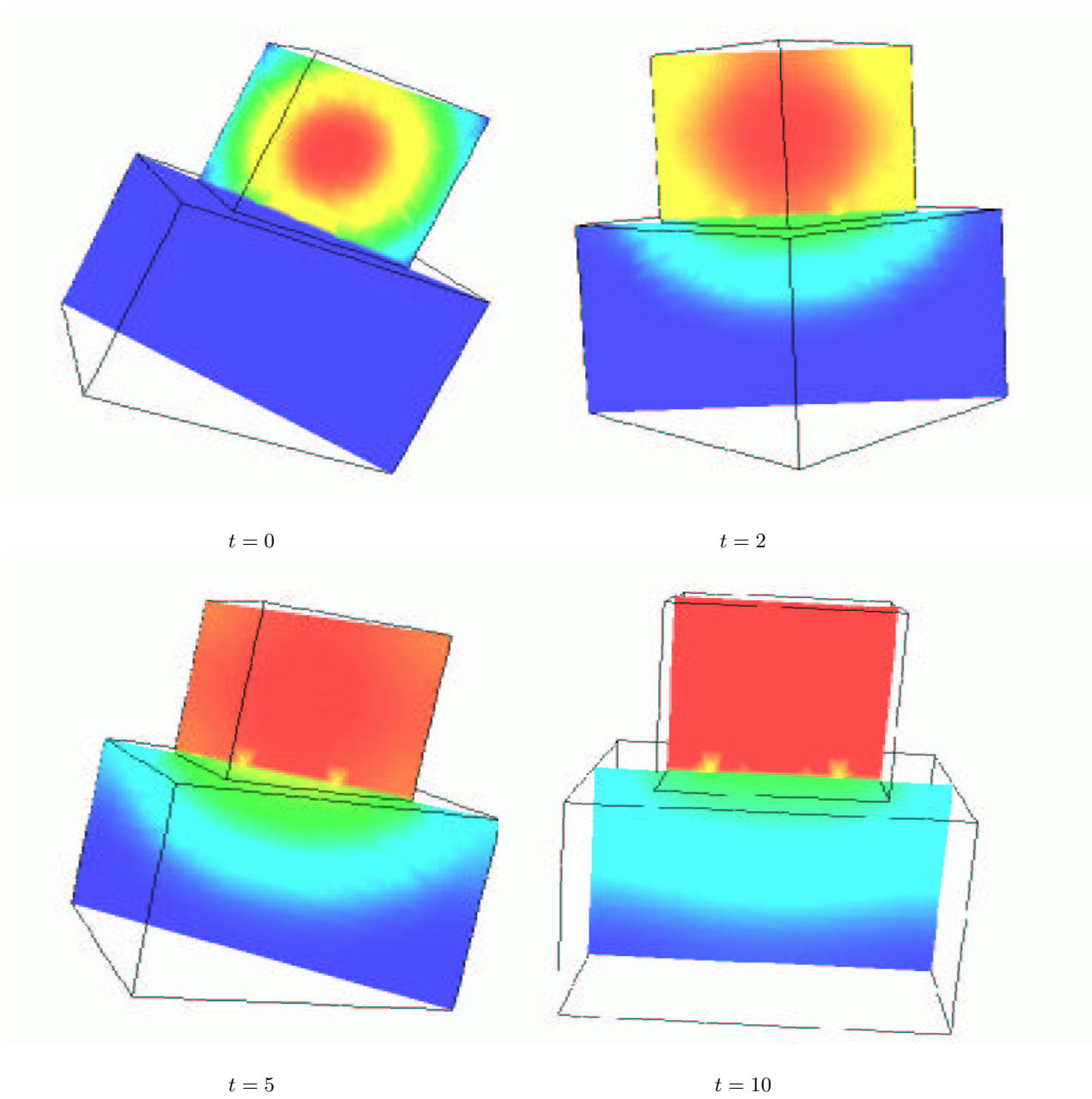$t = 0$ $t = 2$

$t = 5$ $t = 10$

Figure 2: Initial species distribution ($t = 0$) shows higher concentration Gaussian profile in the top cube and lower constant concentration in the bottom cube. Simulation shows that the species penetrates from the top cube into the bottom cube ($t = 2, 5, 10$).

8. References

1. Antoniadis, D.A., Rodoni, M., Dutton, R.W., "Impurity redistribution in SiO2-Si during oxidation: A numerical solution including interfacial fluxes" , *J. Electrochem. Soc. Solid-State Sci. techn.*, vol. 126, pp. 1939-1945, 1979.

2. Lau, F., Mader, L., Mazure, C., Werner, C., and Orlowski, M., "A Model for Phosporus Segregation at the Silicon - Silicon Dioxide Interface", *Appl. Phys. A*, vol. 49, pp. 671-675, 1989.

3. Mulvaney, B.J., Richardson, W.B., and Crandle, T.L., "PEPER - A Process Simulator for VLSI", *IEEE Transactions on Computer Aided Design*, vol. 8, no. 4, pp. 336-348, 1989.

4. Penumalli, B.R., "A Comprehensive Two-Dimensional VLSI Process Simulation Program, BICEPS"', *IEEE Electr. Dev., vol. 3,* pp. 986-992, 1983.

5. Johnson, C., *Numerical solution of partial differential equations by the finite element method.* Cambridge University Press, 1987.

6. Crank, J., *The Mathematics of Diffusion.* Oxford University Press, 1989.